Supplementary Figure 1

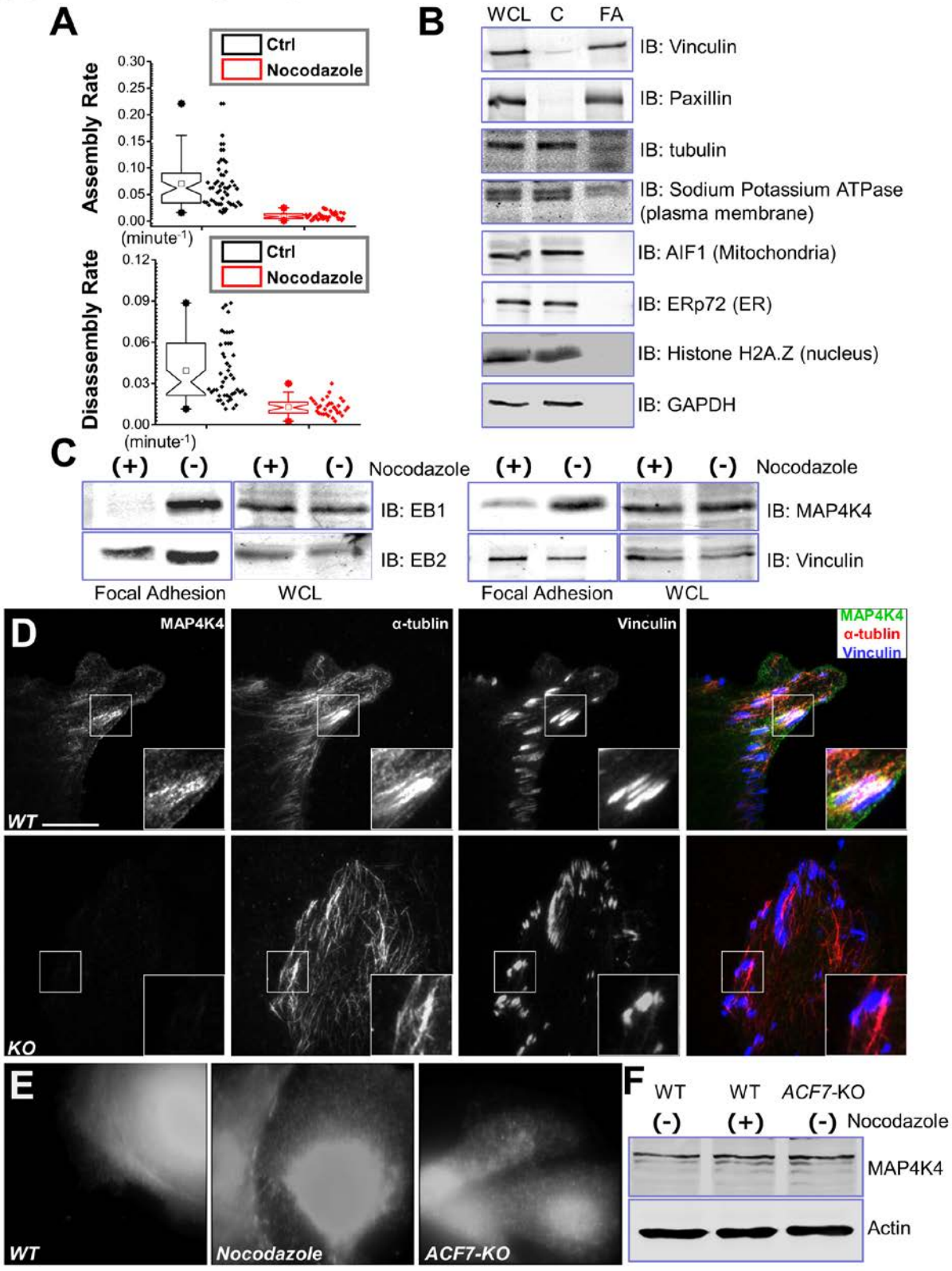

Supplementary Figure 2

A

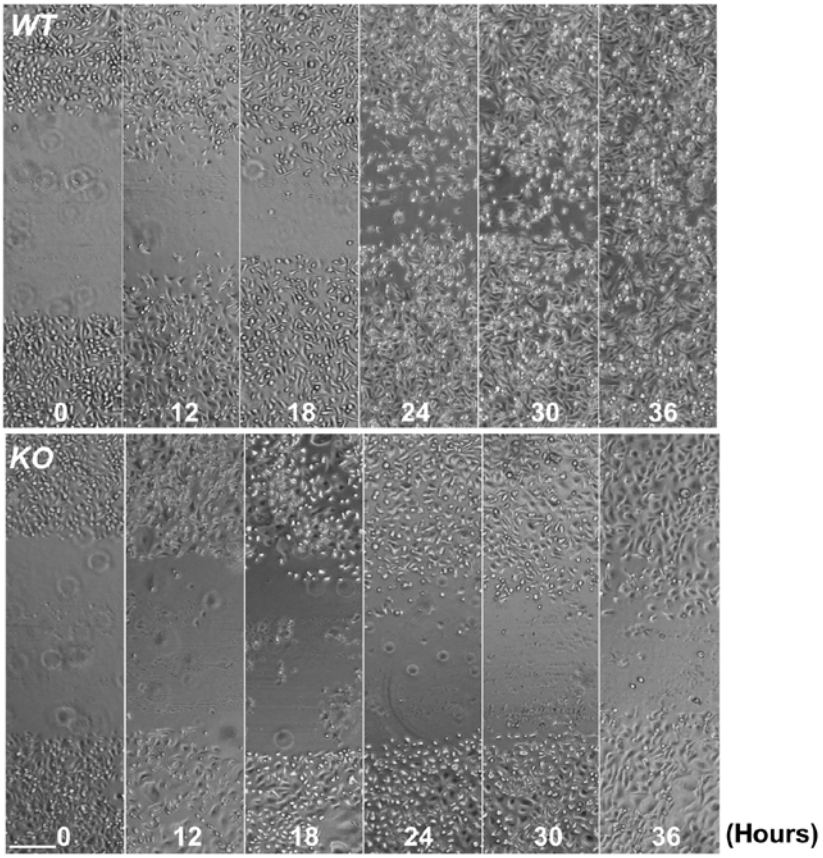

B

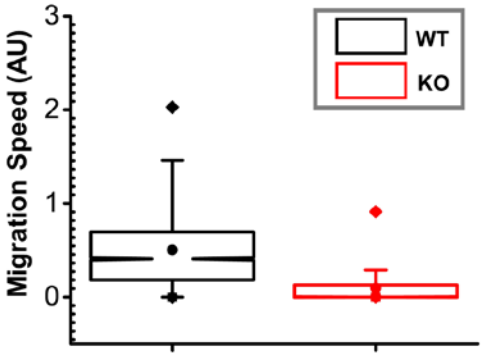

Supplementary Figure 3

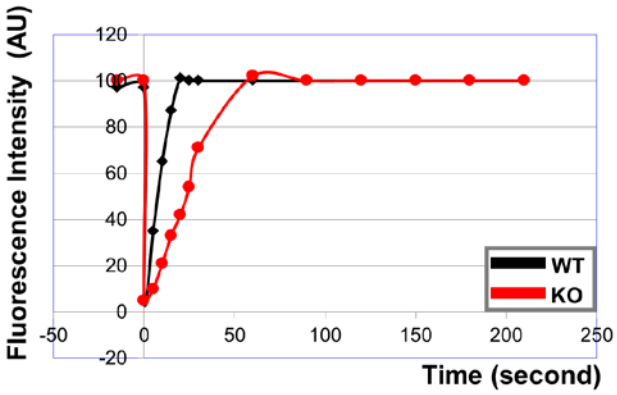

Supplementary Figure 4

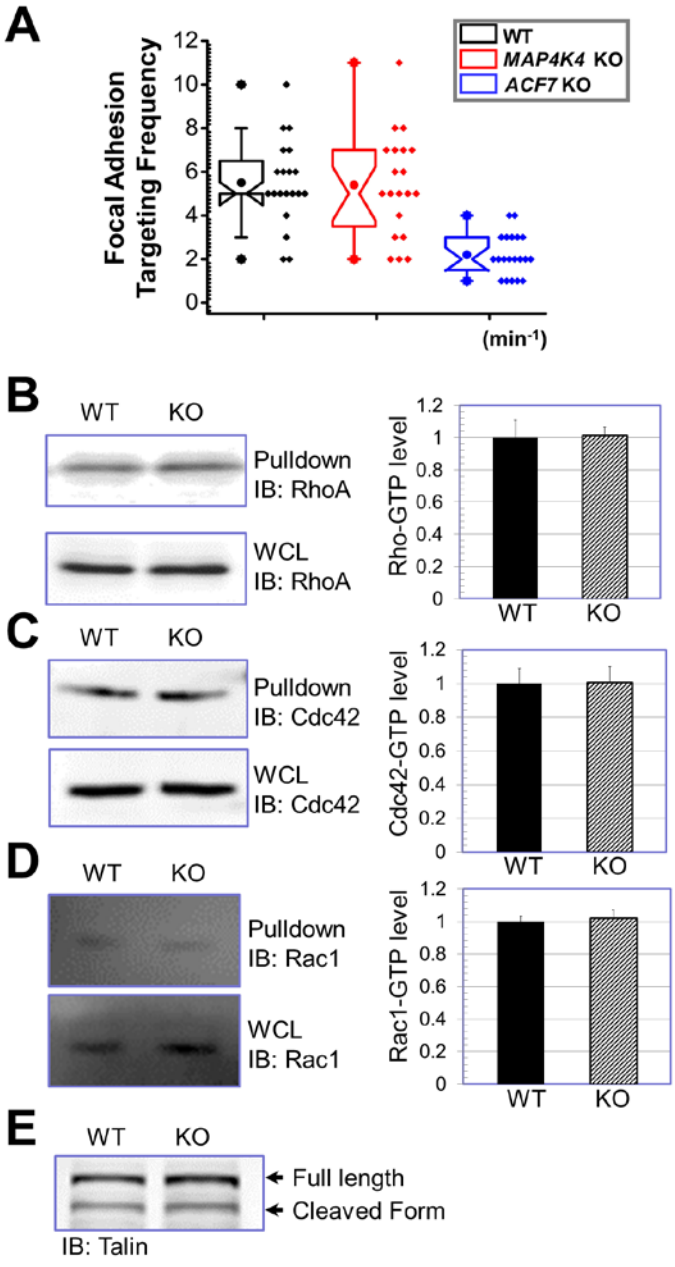

Supplementary Figure 5

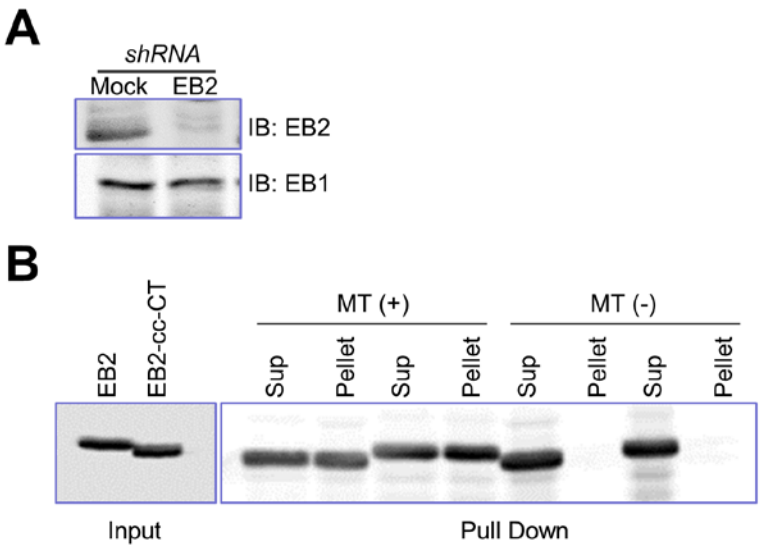

Supplementary Figure 6

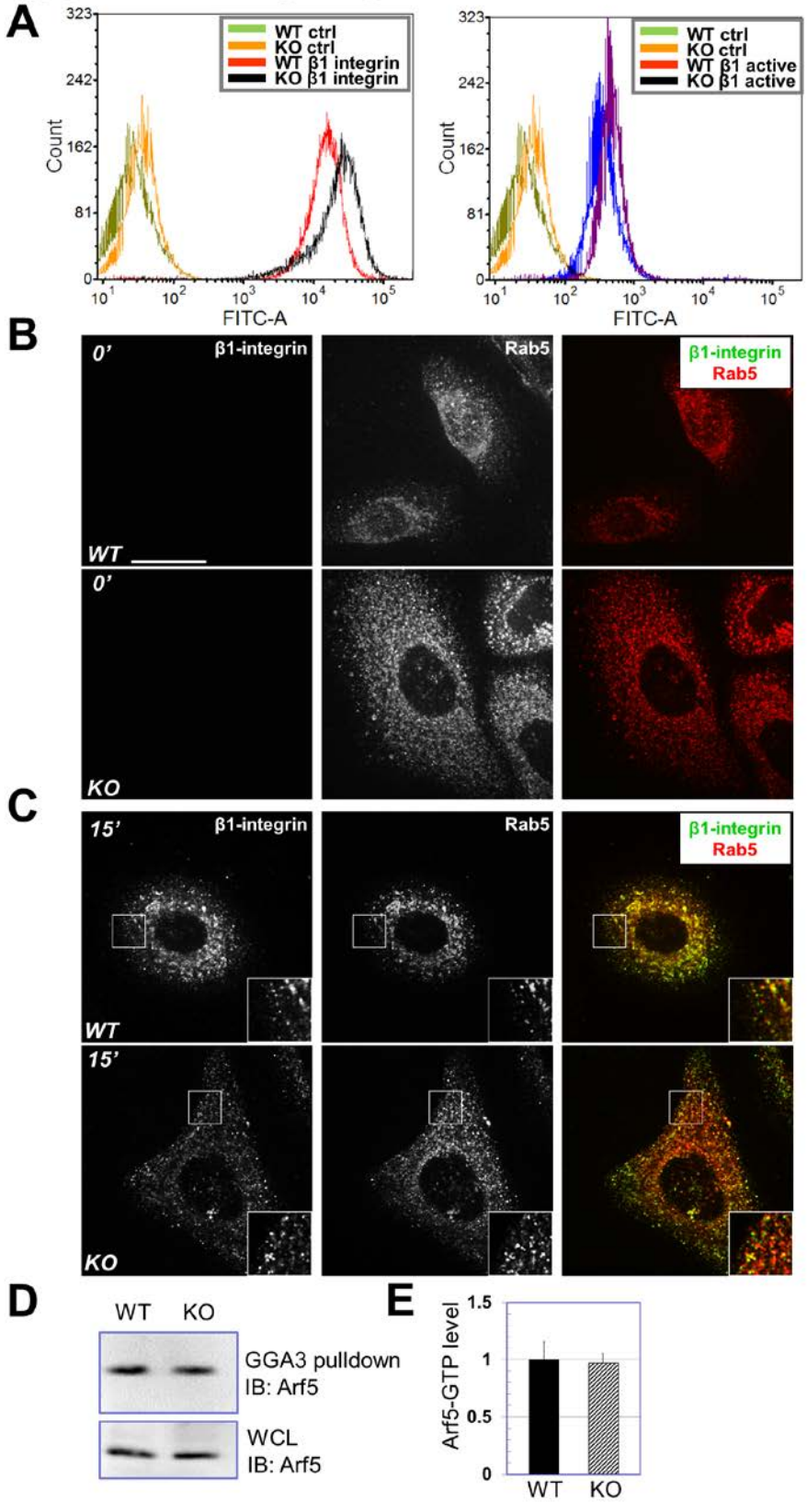

Supplementary Figure 7

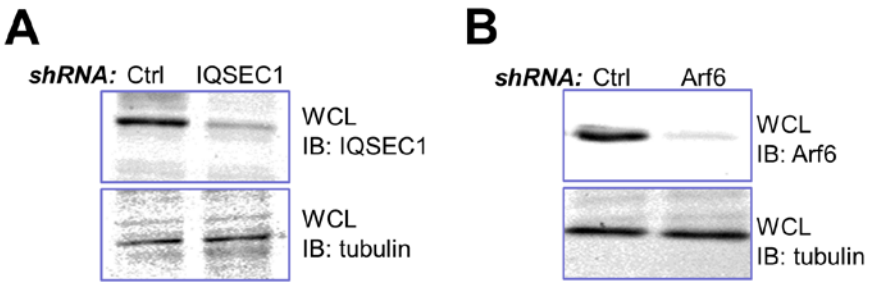

Supplementary Figure Legends

Supplementary Figure 1: Identification of MAP4K4 as a potential MT-associated focal adhesion disassembly factor (related to Fig. 1)**. (A)** Box and whisker plots revealing slow assembly and disassembly rates of focal adhesions in HaCaT cells treated with nocodazole. Box and whisker plots indicate the mean (empty square within the box), 25th percentile (bottom line of the box), median (middle line of the box), 75th percentile (top line of the box), 5th and 95th percentile (whiskers), 1st and 99th percentile (solid diamonds) and minimum and maximum measurements (solid squares), with actual data points shown at right. N>40 for each group, and P<0.01. **(B)** Cell fractions and whole cells lysate (WCL) were subjected to immunoblot (IB) with different antibodies as indicated. C: cytosolic fraction, FA: focal adhesion fraction. Note enrichment of vinculin and paxillin (focal adhesion marker protein) and absence of GAPDH (cytosolic protein), AIF1 (mitochondria marker), ERp72 (ER marker protein), or H2A.Z (nuclear protein) in FA fraction. **(C)** Protein abundance in isolated focal adhesions or whole cell lysate (WCL, 10 μg) from cells treated with or without nocodazole was determined by immunoblot (IB) with different antibodies as indicated. **(D)** WT and *MAP4K4* KO cells were fixed and stained with different antibodies as indicated. Stained cells were examined by TIRF microscopy. Note enrichment of endogenous MAP4K4 at the ends of MT bundles that associate with focal adhesions in WT cells, and loss of MAP4K4 staining in the KO cells. Scale bar represents 20 μm. **(E)** Epi-fluorescence imaging of the same cells shown in Figure 1D. Note comparable level of MAP4K4 in these cells. **(F)** Level of endogenous MAP4K4 in WT keratinocytes, WT keratinocytes treated with nocodazole, and *ACF7* KO keratinocytes was determined by immunoblot. Cell lysates were also blotted with α-actin antibody to verify similar loading.

Supplementary Figure 2: Deletion of *MAP4K4* inhibits cell motility *in vitro* (related to Fig. 2)**. (A)** Migration of confluent monolayers of keratinocytes cultured from *MAP4K4* cKO and WT littermates and subjected to *in vitro* scratch-wound assays. Phase contrast images of the site were taken at hours

indicated after scratch-wounding. Scale bar represents 50 µm. **(B)** Box and whisker plots of WT and *MAP4K4* KO cell velocities *in vitro*. N= 30 cells X 120 time points. P<0.01.

Supplementary Figure 3: FRAP analysis of WT and *MAP4K4* KO cells (related to Fig. 3)**.** A representative example of fluorescence recovery kinetics for WT and *MAP4K4* KO cells after bleaching.

Supplementary Figure 4: MT targeting to focal adhesions, Rho activity, and talin activation in keratinocytes (related to Fig. 4)**. (A)** MT targeting to focal adhesions in WT, *MAP4K4* KO, or *ACF7* KO cells were quantified with confocal videomicroscopy and shown as box-whisker plot. N=20 for each group. P<0.01 between WT and ACF7 KO, and P=0.88 between WT and MAP4K4 KO. **(B-D)** Level of GTP-bound RhoA, Cdc42, and Rac1 in WT and *MAP4K4* KO cells were determined by pull-down assay and quantified by densitometry (right panels). N=3, and P>0.5 for each group. **(E)** Level of talin and cleaved talin in WT and *MAP4K4* KO cells was examined by immunoblot.

Supplementary Figure 5: EB2 knockdown and binding of EB2-cc-CT mutation with MTs (related to Fig. 5)**. (A)** Knockdown expression of endogenous EB2 was achieved by shRNA. Cells treated with control or *EB2* shRNA were subjected to immunoblot with different antibodies as indicated. Note EB2 depletion does not affect stability of other end binding proteins (EB1). **(B)** MT binding of EB2 or EB2-cc-CT mutant was examined by co-sedimentation assay as described.

Supplementary Figure 6: Endocytosis of β1-integrin and Arf5 activity in WT and KO cells (related to Fig. 6)**. (A)** Representative examples of total β1-integrin (left panel) and active β1-integrin (right panel) on cell surface determined by flow cytometry for WT and *MAP4K4* KO cells. **(B-C)** Internalized surface β1-integrin was visualized by immunofluorescence staining of WT and *MAP4K4* KO cells. The cells were co-stained with antibody against Rab5 (early endosome marker). Note internalized integrin after 15 minutes (B) incubation in both WT and KO cells, but not present in the

control cells (0 minute, A). Internalized β1 integrin localizes at Rab5-positve vesicles. Boxed areas are magnified as insets in (B). Note significant co-localization but not identical localization pattern between internalized integrin and Rab5. **(D-E)** Arf5-GTP level was determined by GGA3 pull-down in WT and *MAP4K4* KO cells. For WCL, 20 μg of total proteins were used (A). Level of Arf5 activation was determined by densitometry (B). N=3.

Supplementary Figure 7: Knockdown expression of *Arf6* and *IQSEC1* in mouse keratinocytes (related to Fig. 7)**.** Keratinocytes treated with control or IQSEC1 shRNA **(A)** or Arf6 shRNA **(B)** were subjected to immunoblot with different antibodies as indicated.

Supplementary Table (Spreadsheet): Quantitative analysis of focal adhesion proteome upon nocodazole treatment by SILAC (related to Fig. 1)**.**

Focal adhesion proteins were isolated from control or nocodazole treated keratinocytes after SILAC labeling (Fig. 1A and experimental procedures). All identified proteins with Heavy/Light ratio greater than 1.5 or less than 0.5 are listed in the excel spreadsheet. Protein ID, name, together with sequence information and H/L ratio are shown in the table.

Supplementary Video 1: Focal adhesion dynamics in WT and KO keratinocytes (related to Fig. 3)**.**

WT and KO keratinocytes expressing DsRed-Zyxin were plated on fibronectin (5 μg/ml)-coated dishes. Dynamics of focal adhesion were recorded by confocal spinning-disc videomicroscopy. Images were taken at 2 frames per minute.

Supplementary Video 2: Dynamic localization of EB2 cc-CT mutant (related to Fig. 5)**.**

WT keratinocytes transfected with TagRFP-EB2-cc-CT were plated on fibronectin (5 μg/ml)-coated dishes. Dynamics of EB2 mutant were recorded by confocal spinning-disc videomicroscopy. Images were taken at 1 frame per second.

Supplementary Experimental Procedures

LC-MS/MS analysis

MS analysis was carried out by the proteomics core of University of Chicago. For both SILAC samples and TAP (tandem affinity purification) samples, protein bands were excised by sterile razor blade and chopped into ~1 mm^3 pieces. Each sample was washed in water and destained using 100 mM ammonium bicarbonate pH 7.5 in 50% acetonitrile. A reduction step was performed by addition of 100 µl 50 mM ammonium bicarbonate pH 7.5 and 10 µl of 10 mM Tris(2-carboxyethyl)phosphine HCl at 37°C for 30 min. The proteins were alkylated by adding 100 µl 50 mM iodoacetamide and allowed to react in the dark at 20°C for 30 min. Gel samples were washed in water, then acetonitrile, and dried in a SpeedVac. Trypsin digestion was carried out overnight at 37°C with 1:50 enzyme-protein ratio of sequencing grade-modified trypsin (Promega) in 50 mM ammonium bicarbonate pH 7.5, and 20 mM $CaCl_2$. Peptides were extracted with 5% formic acid and vacuum dried.

The peptide samples were loaded to a 0.25 µl C_8 OptiPak trapping cartridge custom-packed with Michrom Magic C8 (Optimize Technologies), washed, then switched in-line with a 20 cm by 75 µm C_{18} packed spray tip nano column packed with Michrom Magic C18AQ, for a 2-step gradient. Mobile phase A was water/acetonitrile/formic acid (98/2/0.2) and mobile phase B was acetonitrile/isopropanol/water/formic acid (80/10/10/0.2). Using a flow rate of 350 nl/min, a 90 min, 2-step LC gradient was run from 5% B to 50% B in 60 min, followed by 50%–95% B over the next 10 min, hold 10 min at 95% B, back to starting conditions and re-equilibrated. The samples were analyzed via electrospray tandem mass spectrometry (LC-MS/MS) on a Q-Exactive (Thermo scientific) mass spetrometer, using a 60,000 RP survey scan, m/z 375-1950, with lockmasses, followed by 15 HCD CID scans on only doubly and triply charged precursors between 375 Da and 1950 Da. Inclusion lists of expected acetylated or phosphorylated tryptic in-silico peptide ion masses were also used. Ions selected for MS/MS were placed on an exclusion list for 60 seconds.

Tandem mass spectra were extracted by MSConvert (ProteoWizard 3.0.3768) All MS/MS samples were analyzed using MaxQuant (Max Planck Institute of Biochemistry, Martinsried, Germany;

version 1.2.2.5. MaxQuant was set up to search the 140204_SPROT_HUMAN database (unknown version, 47496 entries) also assuming strict trypsin. MaxQuant and X! Tandem were searched with a fragment ion mass tolerance of 20 PPM and a parent ion tolerance of 20PPM. Carbamidomethyl of cysteine was specified in MaxQuant as a fixed modification. Label:2H(4) of lysine, oxidation of methionine, acetyl of the n-terminus, and phospho of serine, threonine and tyrosine were specified in MaxQuant as variable modifications.

Skin Wound Healing

For skin wound healing assays, same sex littermates of ~ 12 wk old mice were anesthetized, and two full-thickness excisional wounds were made on both sides of the dorsal midline (Wu et al., 2008). Mice were housed separately, and no self-induced trauma was observed in control or cKO mice. Tissue was collected 2-6 days after wounding, and wound reepithelialization was evaluated by histological analyses. Hyperproliferative epidermis (HE) was identified by hematoxylin and eosin staining, and the length of HE that extended into the wounds was measured and quantified.

Antibodies, Reagents, and Plasmid DNA Constructions

Rabbit polyclonal antibody against MAP4K4 was obtained from Bethyl Labs (Montgomery, TX). Rat monoclonal antibody against EB1 and EB2 were obtained from Thermo (Waltham, MA). Guinea pig anti K5, rabbit anti K10 and Loricrin antibodies were generous gifts from Dr. Elaine Fuchs at the Rockefeller University. Rat monoclonal β4-integrin (CD104) was obtained from BD Pharmingen (Franklin lakes, NJ). Mouse monoclonal antibodies against pan β1-integrin or activated β1-integrin were obtained from Millipore (Billeria, MA). Mouse monoclonal antibody against IQSEC1 (GEP100) was obtained from GeneScience (Tokyo, Japan). Human plasma fibronectin, nocodazole, taxol, ATP, HA-conjugated Agarose, mouse monoclonal Vinculin, Paxillin, talin, acetylated tubulin, and β-tubulin Abs were obtained from Sigma (St. Louis, MO). Texas Red-conjugated Phalloidin was obtained from Invitrogen (Carlsbad, CA). Mouse monoclonal Abs against Myc, and rabbit polyclonal Abs against HA, Rab5, AIF1, ERp72, sodium potassium ATPase, H2A.Z, and Ki67 were obtained from Santa Cruz

Biotechnology, Inc. (Santa Cruz, CA). Microtubule binding protein spindown kit and Arf6 Pull-down activation assay kit were obtained from Cytoskeleton (Denver, CO). Monoclonal antibody against Arf5 was obtained from Abnova (Walnut, CA). Other chemicals or reagents were obtained from Sigma, unless otherwise indicated. DNA miniprep and other extraction kits were obtained from Zymo Research (Irvine, CA).

Plasmids encoding DsRed-Zyxin, GFP-Paxillin, and EB1 have been described (Kodama et al., 2003; Schober et al., 2007). Full-length *MAP4K4* cDNA was subcloned from Open Biosystem ORF clones (Thermo, clone ID 100068356, encoding isoform 2 of mouse *MAP4K4*) into mammalian expression vectors, pKH3S and pHANS (with N terminal HA or Myc tag). MAP4K4 kinase defective mutant (D153N) was generated by overlapping PCR with primers: AAC TGC AGT TTC GGT GAA TAA CGT GGT GAA TAT G , AAG GAA AAA AGC GGC CGC TCG AGA TGG CGA ACG ACT CTC C. Plasmid encoding full-length *EB2* cDNA was a generous gift from Dr. Yulia Komarova at University of Illinois at Chicago. *EB2* coding sequence was subcloned to other mammalian expression vectors, including pKH3. Mutations in *EB2* were created by over-lapping PCRs with primers: AAG GAA AAA AGC GGC CGC TCA TGG CGG TCA ATG TGT ATT CTA C, GGA ATT CTT AAT ACT CTT CTT GTT CCT CCT GTG GGC CCC CTT CAT CAG GTA TCA CAA AGC CTT CAT CGG AAG CGT AGA GCA C, TCC TAA GGC TGG CCC CGG AAT GGT GCG AAA GAA TCC TGG TGT GGG CAA TGG AGA TGA TGA AGC AGC TGA ACT CAA CGA GCA GGT ACA TTC, CCA CAG AGA CCC ATT GCA ACA CAG AGG ACT ACT GCA GCT CCT AAG GCT GGC CCC GGA ATG, GAA GAT CTT CAA CCT GCC CAA GAA GCC TCT CGG CTC CAG TAC TGC AGC CCC ACA GAG ACC CAT TGC AAC. ShRNA vectors targeting *EB2* and *IQSEC1* were prepared from Decipher shRNA vector (pRSI9-U6-UbiC-TagRFP-2A-Puro) with primers: ACC GGG ATG AAT GTT GAT AAG GTA GTT AAT ATT CAT AGC TAC CTT ATC AAC ATT CAT CTT TTT T, CGA AAA AAA AGA TGA ATG TTG ATA AGG TAG CTA TGA ATA TTA ACT ACC TTA TCA ACA TTC ATC C, ACC GGC CAG TGT TAC TGT TGG CAA ATC TCG AGA TTT GCC AAC AGT AAC ACT GGT TTT TG, CGA ACA AAA ACC AGT GTT ACT GTT GGC AAA TCT CGA GAT TTG CCA ACA GTA ACA CTG G, ACC GGC CTT TCA GAT TGG AAG GAG TTC TCG AGA ACT CCT TCC AAT CTG AAA GGT TTT TG, CGA ACA AAA ACC

TTT CAG ATT GGA AGG AGT TCT CGA GAA CTC CTT CCA ATC TGA AAG GC', ACC GGG AAA GAG AAC TGA TCA CCA TAC TCG AGT ATG GTG ATC AGT TCT CTT TCT TTT TG, CGA ACA AAA AGA AAG AGA ACT GAT CAC CAT ACT CGA GTA TGG TGA TCA GTT CTC TTT CC, ACC GGC TGT CAG CAT GGC TCA TCT TTC TCG AGA AAG ATG AGC CAT GCT GAC AGT TTT TG, CGA ACA AAA ACT GTC AGC ATG GCT CAT CTT TCT CGA GAA AGA TGA GCC ATG CTG ACA GC, ACC GGC CCT TTC AGA TTG GAA GGA GTC TCG AGA CTC CTT CCA ATC TGA AAG GGT TTT TG, CGA ACA AAA ACC CTT TCA GAT TGG AAG GAG TCT CGA GAC TCC TTC CAA TCT GAA AGG GC. Mutation at *EB2* shRNA recognition site was created by overlapping PCR with primers: AGC ATC CTT TAA ACG GAT GAA CGT CGA CAA AGT CAT CCC AGT GGA GAA G, CTT CTC CAC TGG GAT GAC TTT GTC GAC GTT CAT CCG TTT AAA GGA TGC T. Plasmid encoding IQSEC1 (Arf-GEP_{100}) was a generous gift from Dr. Martha Vaughan at National Institutes of Health. IQSEC1 coding sequence was transferred to other mammalian expression vectors, including pKH3S. Plasmid encoding *Arf6* T157A was generated by overlapping PCR with primers: CGC GGA TCC TCA TGT TGG GCC TG, GAT TTG TAG TTA GAG GCT AAC CAT GTG AGC CC, GGG CTC ACA TGG TTA GCC TCT AAC TAC AAA TC, CCG CTC GAG CGG CCG CCA GTG TG.

Histology and Immunofluorescence

Skin or wound samples were embedded in OCT, frozen, sectioned, and fixed in 4% formaldehyde. For paraffin sections, samples were incubated in 4% formaldehyde at 4°C overnight, dehydrated with a series of increasing concentrations of ethanol and xylene, and then embedded in paraffin. Paraffin sections were rehydrated in decreasing concentrations of ethanol and subjected to antigen unmasking in 10 mM Citrate, pH 6.0. Sections were subjected to hematoxylin and eosin staining or immunofluorescence staining as described (Guasch et al., 2007). Antibodies were diluted according to manufacturer's instruction, unless indicated.

For immunofluorescence staining of cells, keratinocytes were fixed and stained with different primary and secondary antibodies as indicated. Pictures were acquired on a fluorescence microscope on a 16-bit scale. To examine β1-integrin endocytosis, we carried out treatment and

immunofluorescence staining essentially as described (Wu et al., 2005). Briefly, cells were incubated with β1-integrin antibody at 4°C for 30 minutes and then cultured at 37°C for 15 minutes to allow surface receptor internalization. Cells were then washed with ice-cold PBS and then with stripping buffer (0.2M HAc, 0.5M NaCl, pH2.8) at 4°C for 30 minutess. After fixation, cells were stained with antibodies against integrin and Rab5. Images were taken on Marianas spinning dish confocal microscope.

Microtubule Pull Down Assay, Arf6 Pull Down Assay, and other biochemical analysis

Microtubule binding were examined using microtubule binding protein spin-down assay kit from Cytoskeleton (Denver, CO), according to manufacturer's instructions. Arf6 pull-down activation assay (GGA3 pull down) was performed according to manufacturer's instruction (Cytoskeleton, Denver, CO). Rho family GTPases pulldown assay was done following the instructions of RhoA/Rac1/Cdc42 activation assay kit (Cytoskeleton, Denver, CO). Immunoprecipitation and western blotting were performed as described previously (Wu et al., 2004). Tandem affinity purification was performed essentially as described (Wu et al., 2007). Protein phosphorylation was determined by phos-tag reagent (Wako pure Chemical Industries, Japan) according to manufacturer's instruction.

Integrin endocytosis assay was performed as previously described (Wu et al., 2005). In brief, cells were washed with ice-cold PBS. Cell membrane proteins were labelled with 0.2 mg/ml Sulfo-NHS-SS Biotin in PBS. After incubation at 37°C for the indicated time points, cells were treated with reduction buffer (42mM glutathione reduced form, 75mM NaCl, 1mM EDTA, 1% BSA, 75mM NaOH) for 20mins on ice twice. Biotinylated proteins were pull-downed with streptavidin beads from lysed cell lysates and examined by Western Blot. Transferrin receptor was used as an internal control for the assay (Wu et al., 2005).

The acrylamide-pendant Phos-tag ligand provides a phosphate affinity SDS-PAGE for mobility shift detection of protein phosphorylation. This methodology has now been well established and served as an excellent alternative approach for radioisotope-free detection of protein phosphorylation (Humke et al., 2010; Matos et al., 2008; Ydenberg and Rose, 2009).

Supplementary references

Guasch, G., Schober, M., Pasolli, H.A., Conn, E.B., Polak, L., and Fuchs, E. (2007). Loss of TGFbeta signaling destabilizes homeostasis and promotes squamous cell carcinomas in stratified epithelia. Cancer Cell *12*, 313-327.

Humke, E.W., Dorn, K.V., Milenkovic, L., Scott, M.P., and Rohatgi, R. (2010). The output of Hedgehog signaling is controlled by the dynamic association between Suppressor of Fused and the Gli proteins. Genes & development *24*, 670-682.

Kodama, A., Karakesisoglou, I., Wong, E., Vaezi, A., and Fuchs, E. (2003). ACF7: an essential integrator of microtubule dynamics. Cell *115*, 343-354.

Matos, J., Lipp, J.J., Bogdanova, A., Guillot, S., Okaz, E., Junqueira, M., Shevchenko, A., and Zachariae, W. (2008). Dbf4-dependent CDC7 kinase links DNA replication to the segregation of homologous chromosomes in meiosis I. Cell *135*, 662-678.

Schober, M., Raghavan, S., Nikolova, M., Polak, L., Pasolli, H.A., Beggs, H.E., Reichardt, L.F., and Fuchs, E. (2007). Focal adhesion kinase modulates tension signaling to control actin and focal adhesion dynamics. J Cell Biol *176*, 667-680.

Wu, X., Gan, B., Yoo, Y., and Guan, J.L. (2005). FAK-mediated src phosphorylation of endophilin A2 inhibits endocytosis of MT1-MMP and promotes ECM degradation. Dev Cell *9*, 185-196.

Wu, X., Kodama, A., and Fuchs, E. (2008). ACF7 regulates cytoskeletal-focal adhesion dynamics and migration and has ATPase activity. Cell *135*, 137-148.

Wu, X., Suetsugu, S., Cooper, L.A., Takenawa, T., and Guan, J.L. (2004). Focal adhesion kinase regulation of N-WASP subcellular localization and function. The Journal of biological chemistry *279*, 9565-9576.

Wu, Y., Li, Q., and Chen, X.Z. (2007). Detecting protein-protein interactions by Far western blotting. Nat Protoc *2*, 3278-3284.

Ydenberg, C.A., and Rose, M.D. (2009). Antagonistic regulation of Fus2p nuclear localization by pheromone signaling and the cell cycle. The Journal of cell biology *184*, 409-422.